

Synthesis and characterization of new 1,3,4-thiadiazole derivatives: study of their antibacterial activity and CT-DNA binding

Hakan Sayiner, Mehmet Yilmazer, Aisha. Abdelsalam, Mohamed Ganim, Cengiz Baloglu, Yasemin Celik Altunoglu, Mahmut Gür, Murat Saracoglu, Mohamed Attia, Safwat Mahmoud, et al.

▶ **To cite this version:**

Hakan Sayiner, Mehmet Yilmazer, Aisha. Abdelsalam, Mohamed Ganim, Cengiz Baloglu, et al.. Synthesis and characterization of new 1,3,4-thiadiazole derivatives: study of their antibacterial activity and CT-DNA binding. RSC Advances, 2022, 12 (46), pp.29627-29639. 10.1039/D2RA02435G . hal-03835355

HAL Id: hal-03835355
https://hal.science/hal-03835355

Submitted on 31 Oct 2022

HAL is a multi-disciplinary open access archive for the deposit and dissemination of scientific research documents, whether they are published or not. The documents may come from teaching and research institutions in France or abroad, or from public or private research centers.

L'archive ouverte pluridisciplinaire **HAL**, est destinée au dépôt et à la diffusion de documents scientifiques de niveau recherche, publiés ou non, émanant des établissements d'enseignement et de recherche français ou étrangers, des laboratoires publics ou privés.



Distributed under a Creative Commons Attribution - NonCommercial 4.0 International License

RSC Advances

PAPER

View Article Online
View Journal | View Issue

Check for updates

Cite this: *RSC Adv.*, 2022, **12**, 29627

Synthesis and characterization of new 1,3,4-thiadiazole derivatives: study of their antibacterial activity and CT-DNA binding

Hakan S. Sayiner,[a] Mehmet I. Yilmazer,[b] Aisha. T. Abdelsalam,[c] Mohamed A. Ganim,[c] Cengiz Baloglu,[c] Yasemin Celik Altunoglu,[c] Mahmut Gür,[d] Murat Saracoglu,*[b] Mohamed S. Attia,*[e] Safwat A. Mahmoud,*[f] Ekram H. Mohamed,[g] Rabah Boukherroub,[h] Nora Hamad Al-Shaalan,[i] Sarah Alharthi,[j] Fatma Kandemirli*[k] and Mohammed A. Amin*[j]

1,3,4-Thiadiazole molecules (**1–4**) were synthesized by the reaction of phenylthiosemicarbazide and methoxy cinnamic acid molecules in the presence of phosphorus oxychloride, and characterized with UV, FT-IR, ^{13}C-NMR, and ^{1}H-NMR methods. DFT calculations (b3lyp/6-311++G(d,p)) were performed to investigate the structures' geometry and physiochemical properties. Their antibacterial activity was screened for various bacteria strains such as *Enterobacter aerogenes*, *Escherichia coli* ATCC 13048, *Salmonella kentucky*, *Pseudomonas aeruginosa*, *Klebsiella pneumoniae*, *Proteus* and Gram positive such as *Staphylococcus aureus* ATCC 25923, *Listeria monocytogenes* ATCC 7644, *Enterococcus faecium*, *Enterococcus durans*, *Staphylococcus aureus* ATCC, *Serratia marcescens*, *Staphylococcus hominis*, *Staphylococcus epidermidis*, alfa *Streptococcus haemolyticus*, *Enterococcus faecium* and found to have an inhibitory effect on *Klebsiella pneumoniae* and *Staphylococcus hominis*, while molecules **1**, **3** and **4** had an inhibitory effect on *Staphylococcus epidermidis* and alpha *Streptococcus haemolyticus*. The experimental results were supported by the docking study using the Kinase ThiM from *Klebsiella pneumoniae*. All the investigated compounds showed an inhibitory effect for the *Staphylococcus epidermidis* protein. In addition, the mechanism of the **1–4** molecule interaction with calf thymus-DNA (CT-DNA) was investigated by UV-vis spectroscopic methods.

Received 15th April 2022
Accepted 26th September 2022

DOI: 10.1039/d2ra02435g

rsc.li/rsc-advances

Open Access Article. Published on 17 October 2022. Downloaded on 10/31/2022 3:10:04 PM.
This article is licensed under a Creative Commons Attribution-NonCommercial 3.0 Unported Licence.

1 Introduction

Heterocyclic molecules are cyclic compounds comprising carbon and other elements such as oxygen, nitrogen and sulphur. The heterocyclic molecules containing a single heteroatom are pyrrole, furan and thiophene, while those consisting of more than one heteroatom are azole, pyrrole, thiazole, thiadiazole, oxadiazole, triazene *etc.*[1] There are many different heterocyclic molecules that have therapeutic significance. Lately, thiadiazole derivatives have become an important field of research due to their broad-spectrum activities. Thiadiazoles belong to the classes of nitrogen–sulfur containing heterocycles with extensive application as structural units of biologically active molecules and are useful intermediates in medicinal chemistry. There are four possible structures of thiadiazole such as 1,2,5-thiadiazole, 1,3,4-thiadiazole, 1,2,3-thiadiazole and 1,2,4-thiadiazole, but 1,3,4-thiadiazole is the most versatile owing to its pharmacological and biological activities (Fig. 1).[2] During the past years, substituted 1,3,4-thiadiazole derivatives have received significant attention and have been increasingly investigated due to their broad spectrum of pharmacological properties.[2] It is supposed that 1,3,4-thiadiazole derivatives

[a]*Department of Infectious Diseases, Faculty of Medicine, Adiyaman University, Adiyaman, Turkey*
[b]*Faculty of Education, Erciyes University, 38039, Kayseri, Turkey. E-mail: muratsaracoglu@gmail.com*
[c]*Department of Genetic & Bioengineering, Faculty of Engineering & Architecture, Kastamonu University, 37150, Kastamonu, Turkey*
[d]*Department of Forest Industrial Engineering, Faculty of Forestry, Kastamonu University, 37150, Kastamonu, Turkey*
[e]*Chemistry Department, Faculty of Science, Ain Shams University, Abbassia 11566, Cairo, Egypt. E-mail: mohd_mostafa@sci.asu.edu.eg*
[f]*Physics Department, Faculty of Science, Northern Border University, Arar, Saudi Arabia*
[g]*Department of Analytical Chemistry, Faculty of Pharmacy, The British University in Egypt, 11837, El-Sherouk City, Egypt*
[h]*Univ. Lille, CNRS, Centrale Lille, Univ. Polytechnique Hauts-de-France, UMR 8520 – IEMN, F59000 Lille, France*
[i]*Department of Chemistry, College of Science, Princess Nourah Bint Abdulrahman University, P.O. Box 84428, Riyadh 11671, Saudi Arabia*
[j]*Department of Chemistry, College of Science, Taif University, P.O. Box 11099, Taif 21944, Saudi Arabia. E-mail: mohamed@tu.edu.sa*
[k]*Department of Biomedical Engineering, Faculty of Engineering and Architecture, Kastamonu University, 37150, Kastamonu, Turkey. E-mail: fkandemirli@yahoo.com*

© 2022 The Author(s). Published by the Royal Society of Chemistry



Fig. 1 Chemical structure of thiadiazole isomers.

Open Access Article. Published on 17 October 2022. Downloaded on 10/31/2022 3:10:04 PM.
This article is licensed under a Creative Commons Attribution-NonCommercial 3.0 Unported Licence.

exhibit various biological activities due to the presence of =N–C–S– moiety.[2] Other authors assume that the biological activities of 1,3,4-thiadiazole derivatives are due to the strong aromaticity of the ring, which also provides great *in vivo* stability to this five-membered ring system and low toxicity for higher vertebrates, including human beings.[3]

Thiadiazole contains both a sulphur atom and two nitrogen atoms as part of its aromatic five-membered ring and has a "hydrogen bonding domain" and "two-electron donor system" functions as anhydrase.[3]

Among the thiadiazole isomers, our attention was focused on 1,3,4-thiadiazole. The importance of 1,3,4-thiadiazole originates from its biological activity, featuring antimicrobial,[4,5] antituberculosis,[6] anti-inflammatory,[7,8] carbonic anhydrase inhibitor,[9] anticonvulsants,[10,11] antihypertensive,[12,13] antioxidant,[14] anticancer,[15,16] and antifungal[17] properties. 1,3,4-Thiadiazole derivatives are important precursors in various chemical reactions for the synthesis of biologically-active molecules. Some examples of drug molecules that comprise 1,3,4-thiadiazole group in their structure are: acetazolamide and methazolamide as carbonic anhydrase inhibitors.[9] It was reported that the thiadiazole group could act as the bio-isosteric substitute of the thiazole moiety.[18] The biological activity of thiadiazole derivatives is due to their strong aromaticity. For higher vertebrates including humans, thiadiazole showed little or no toxicity effect.[19]

Farghaly *et al.*[20] synthesized a series of 1,3,4-thiadiazoles, investigated their antimicrobial activity, and studied their structure activity relationship (SAR) towards some microorganisms. The results of this study revealed that this class of molecules holds promising activity. Bhatia *et al.*[21] prepared various imidazo-thiadiazole derivatives, and screened their antimicrobial activity. The results revealed that these molecules are active against *Shigella flexneri*, *Staphylococcus aureus* (*S. aureus*) and *Candida albicans* bacterial strains. Kaur *et al.*[17] synthesized biphenyl imidazo[2,1-*b*][1,3,4]thiadiazole derivatives and found that these molecules exhibit moderate to good activity when compared with standard antibiotics ampicillin and amphotericin B, and screened the two derivatives for anticancer activity. Gür *et al.*[14] synthesized a series of 1,3,4-thiadiazole derivatives and reported that some of them had effective antioxidant properties.

In this study, 1,3,4-thiadiazole derivatives were synthesized and their antibacterial activity was assessed on both Gram-positive and Gram-negative bacteria. In addition, their antifungal property was assessed for *Candida albicans* ATCC 26555. Besides, interaction of **1–4** molecules and calf thymus DNA (CT-DNA) in physiological buffer (pH = 7.4) was studied by UV-vis absorption to understand the mechanism of interaction of molecules studied with nucleic acids.

2 Experimental section

2.1 Materials and methods

Solvents are distilled and dried before use. Infrared spectra were recorded on FT-IR Fourier Transform Infrared Spectroscopy. ^{13}C and ^{1}H-NMR spectra were acquired on Bruker AVANCE III 400 MHz NMR Spectrometer. Melting points were uncorrected and recorded on SMP30 melting point apparatus. UV-vis absorption spectra were performed by Thermo Scientific MULTISKAN GO spectrophotometer. Quartz cuvettes with 1 cm light path were used in the measurements.

2.2 Synthesis

2.2.1 General procedure for synthesize of thiadiazole derivatives. Equal molar number of phenylthiosemicarbazide and methoxy cinnamic acid derivatives were kept in the refrigerator. Then 3 mmol of phosphorus oxychloride was added dropwise to the mixture of phenylthiosemicarbazide derivatives and methoxy cinnamic acid, and refluxed for 2 h. After cooling to room temperature, ice was added to the mixture. After neutralization with ammonia solution, the obtained product was filtered and washed with water.

*2.2.1.1 5-[(E)-2-(3-Methoxyphenyl)]vinyl-N-[4′-nitrophenyl]-1,3,4-thiadiazole-2-amine (**1**).* Melting point (m.p.): 252 °C. R_f (formic acid : ethylacetate : xylene, 1 : 4 : 5): 0.60. IR ν (cm^{-1}): 3262 (N–H), 3167 (Ar C–H), 1598 (Ar C=C), 1623 (alkene C=C), 1255 (C–N), 1575 (C=N), 1187 (C–S). ^{1}H-NMR (ppm, DMSO-d$_6$): δ = 9.94 (N–H), δ = 8.43–7.00 (m, aromatic protons), δ = 6.95, 6.96 (alkenic protons, overlapped), δ = 3.87 (s, CH_3O protons). ^{13}C-NMR (ppm, DMSO-d$_6$): δ = 55.9 (1C, –OCH_3), δ = 164.0 and 159.4 (2C, thiadiazole carbons), δ = 119.8–157.4 (10C, aromatic carbons), δ = 111.4 and 111.9 (alkenic carbons). UV-vis spectrum: λ_{max} = 241, 368 nm. Elemental analysis (%) for $C_{17}H_{14}N_4O_3S$, experimental (calc.): C = 57.29 (57.62); H = 3.83 (3.98); N = 14.94 (15.81); S = 9.09 (9.05).

*2.2.1.2 5-[(E)-2-(2-Methoxyphenyl)]vinyl-N-[4′-nitrophenyl]-1,3,4-thiadiazole-2-amine (**2**).* M.p.: 247–249 °C. R_f (formic acid : ethylacetate : xylene, 1 : 4 : 5): 0.66. IR ν (cm^{-1}): 3262 (N–H), 3161 (Ar C–H), 1596 (Ar C=C), 1617 (alkene C=C), 1245 (C–N), 1568 (C=N), 1188 (C–S). ^{1}H-NMR (ppm, DMSO-d$_6$): δ = 9.95 (N–H), δ = 8.41–7.02 (m, aromatic protons), δ = 6.88, 6.90 (alkenic protons, overlapped), δ = 3.86 (s, CH_3O protons). ^{13}C-NMR (ppm, DMSO-d$_6$): δ = 55.58 (1C, –OCH_3), δ = 164.2 and 160.1

© 2022 The Author(s). Published by the Royal Society of Chemistry

Open Access Article. Published on 17 October 2022. Downloaded on 10/31/2022 3:10:04 PM. This article is licensed under a Creative Commons Attribution-NonCommercial 3.0 Unported Licence.

(2C, thiadiazole carbons), δ = 115.4–158.9 (10C, aromatic carbons), δ = 111.5 and 112.4 (alkenic carbons). UV-vis spectrum bands: λ_{max} = 243, 267, 374 nm. Elemental analysis (%) for $C_{17}H_{14}N_4O_3S$, experimental (calc.): C = 57.45 (57.62); H = 3.83 (3.98); N = 14.91 (15.81); S = 8.78 (9.05).

*2.2.1.3 5-[(E)-2-(3-Methoxyphenyl)]vinyl-N-[4′-methylphenyl]-1,3,4-thiadiazole-2-amine (**3**).* M.p.: 172–176 °C. R_f (formic acid : ethylacetate : xylene: 1 : 4 : 5): 0.62. IR ν (cm^{-1}): 3247 (N–H), 3114 (Ar C–H), 1596 (Ar C=C), 1235 (C–N), 1548 (C=N), 1183 (C–S), 2953, 2917, 2834 (aliphatic, C–H). ^{1}H-NMR (ppm, DMSO-d_6): δ = 10.45 (N–H), δ = 7.72–7.00 (m, aromatic protons), δ = 6.98, 6.97 (overlapped, alkenic protons), δ = 3.88 (s, CH_3O protons), δ = 2.27 (s, CH_3 protons). ^{13}C-NMR (ppm, DMSO-d_6): δ = 56.1 (1C, –OCH_3), δ = 163.5 and 158.4 (2C, thiadiazole carbons), δ = 120.0–157.4 (10C, aromatic carbons), δ = 112.0 and 118.2 (alkenic carbons). UV-vis spectrum bands λ_{max} = 245, 276, 353 nm. Elemental analysis (%) for $C_{18}H_{17}N_3OS$, experimental (calc.): C = 65.83 (66.85); H = 5.05 (5.30); N = 12.14 (12.99); S = 9.06 (9.91).

*2.2.1.4 5-[(E)-2-(2-Methoxyphenyl)]vinyl-N-[4′-methylphenyl]-1,3,4-thiadiazole-2-amine (**4**).* M.p.: 185 °C. R_f (formic acid : ethylacetate : xylene: 1 : 4 : 5): 0.74. IR ν (cm^{-1}): 3243 (N–H), 3121 (Ar C–H), 1566 (Ar C=C), 1613 (alkene C=C), 1237 (C–N), 1566 (C=N), 1190 (C–S), 2914, 2834 (aliphatic, C–H). ^{1}H-NMR (ppm, DMSO-d_6): δ = 10.47 (N–H), δ = 7.55–7.16 (m, aromatic protons), δ = 6.92, 6.90 (d, alkenic protons), δ = 3.80 (s, methoxy protons); δ = 2.27 (s, methyl protons). ^{13}C-NMR (ppm, DMSO-d_6): δ = 55.6 (1C, –OCH_3), δ = 163.8 and 160.1 (2C, thiadiazole carbons), δ = 118.2–158.0 (10C, aromatic carbons), δ = 112.3 and 115.5 (alkenic carbons). UV-vis spectrum bands: λ_{max} = 242, 274, 358 nm. Elemental analysis (%) for $C_{18}H_{17}N_3OS$, experimental (calc.): C = 65.97 (66.85); H = 4.89 (5.30); N = 12.51 (12.99); S = 9.93 (9.91).

2.3 Enterobacter aerogenes

The antifungal activity of 1,3,4-thiadiazoles was tested on *Candida albicans* ATCC 26555 and their antibacterial activity was evaluated on Gram-negative such as *Enterobacter aerogenes Escherichia coli* ATCC 13048, *Salmonella kentucky*, *Pseudomonas aeruginosa*, *Klebsiella pneumoniae*, *Proteus* and Gram-positive strains such as *Staphylococcus aureus* ATCC 25923, *Listeria monocytogenes* ATCC 7644, *Enterococcus faecium*, *Enterococcus durans*, *Staphylococcus aureus* ATCC, *Serratia marcescens*, *Staphylococcus hominis*, *Staphylococcus epidermidis*, alfa *Streptococcus haemolyticus*, *Enterococcus faecium*. Antifungal activity of 1,3,4-thiadiazoles was assessed on *Candida albicans* ATCC 26555. Standard and other strains were provided from Kastamonu University and Gazi University.

2.4 Antimicrobial activity

All bacterial strains were incubated at 37 ± 2 °C for 24 h and inocula were prepared by transferring morphologically similar colonies of each organism into 0.9% sterile saline solution until the visible turbidity was equal to 0.5 McFarland standard corresponding approximately 10^8 cfu mL^{-1}. 1000 mL of medium was autoclaved at 120 °C for 20 min, then placed in sterile Petri dishes. The prepared bacterial suspension was distributed over the sterile agar surface by rubbing the sterile swab. Before the discs were applied, the inoculated plates were allowed to dry at room temperature for 5–10 min.

Sterile discs filled with solutions containing **1–4** molecules at a concentration of 2 ppm were placed on the surface of inoculated Petri dish. After placing the discs on each plate, it was lightly pressed to make contact with the agar surface and incubated at 37 °C for 24 h. Antibacterial activity against organisms was recorded in mm units after 24 h by measurement of the zone of inhibition. All tests were repeated three times each. After the operations were completed, the plates were sterilized in an autoclave at 120 °C for 20 min and then disposed.[22,23]

2.5 CT-DNA binding experiments

Absorption spectra measurements were conducted using various CT-DNA concentrations (0–90 μM) and keeping the concentration of molecules **1–4** constant (40 μM). The samples were mixed for 30 min at 37 °C.[24] Nucleotide concentration was determined at 260 nm by UV-vis absorption spectroscopy using a molar absorption coefficient of 6600 M^{-1} cm^{-1}.[25]

Molecules **1–4** were prepared at a concentration of 500 μM in DMSO/Tris HCl (65%/35%). The (K) value, known as the binding constant of small molecules with DNA, can be determined by using the Benesi–Hildebrand eqn (1).[26]

$$\frac{A_0}{(A-A_0)} = \frac{\varepsilon_G}{(\varepsilon_{H-G}-\varepsilon_G)} \times \frac{1}{K[\text{CT-DNA}]} + \frac{\varepsilon_G}{(\varepsilon_{H-G}-\varepsilon_G)} \quad (1)$$

where ε_G is the absorption coefficient of the molecule and ε_{H-G} is the absorption coefficient of the DNA molecule, A_0 is the absorbance of the molecule, A is the absorbance of the molecule with DNA, K is the association/binding constant. K can be deduced from the intercept-to-slope ratios of $\frac{A_0}{(A-A_0)}$ *vs.* $\frac{1}{[\text{CT-DNA}]}$ plots.

The intercept-to-slope ratios of the plot of [DNA] *vs.* $\frac{[\text{CT-DNA}]}{(\varepsilon_a-\varepsilon_f)}$ gives also the K value. Where ε_a (or ε_G) is the absorption coefficient of the molecule and ε_f (or ε_{H-G}) is the absorption of the complex obtained through the interaction of the molecule with CT-DNA.[16]

The interaction of thiadiazole derivatives with CT-DNA was examined by calculating the intrinsic binding constant (K) between molecules **1–4** and CT-DNA using the following eqn (2):

$$\frac{[\text{CT-DNA}]}{(\varepsilon_a-\varepsilon_f)} = \frac{[\text{CT-DNA}]}{(\varepsilon_b-\varepsilon_f)} + \frac{1}{K_b(\varepsilon_b-\varepsilon_f)} \quad (2)$$

where ε_a, ε_f, ε_b are respectively the extinction coefficients of the apparent molecule, free molecule, and bound molecule, [DNA] is the concentration of DNA.

ε_f was calculated using the calibration curve generated from the absorbance of molecules **1–4** in aqueous solution, following Beer's law. ε_a was determined as the ratio between the

Open Access Article. Published on 17 October 2022. Downloaded on 10/31/2022 3:10:04 PM.
This article is licensed under a Creative Commons Attribution-NonCommercial 3.0 Unported Licence.

molecules **1–4** concentration and the measured absorbance, A_{obs}/[molecules **1–4**].

A plot of $\frac{[\text{CT-DNA}]}{(\varepsilon_a - \varepsilon_f)}$ *vs.* [CT-DNA] gives a slope of $\frac{1}{(\varepsilon_b - \varepsilon_f)}$ and a *y*-intercept equals to $\frac{1}{K_b(\varepsilon_b - \varepsilon_f)}$.[13]

2.5.1 Computational details. The structure of compounds **1–4** were optimized using Gaussian09 program[26,27] and visualized by Gaussian view 6. All the investigated structures were optimized by b3lyp/6-311++G(d,p) level of theory. The frequency calculations were performed to confirm the structures stability. The reactivity parameters of the compounds **1–4** such as chemical hardness (η), electron donating power (ω^-), and electron acceptor power (ω^+) were calculated from the ionization potential and the electron affinity using eqn (3) and (4):

$$\text{IP} = -E_{\text{HOMO}} \quad (3)$$

$$\text{EA} = -E_{\text{LUMO}} \quad (4)$$

The chemical hardness, electron donating power (ω^-), and electron acceptor power (ω^+) were calculated using eqn (5)–(7):[28]

$$\eta = \frac{1}{2}(\text{IP} - \text{EA}) \quad (5)$$

$$\omega^- = \frac{(3\text{IP} + \text{EA})^2}{16(\text{IP} - \text{EA})} \quad (6)$$

$$\omega^+ = \frac{(\text{IP} + 3\text{EA})^2}{16(\text{IP} - \text{EA})} \quad (7)$$

The molecular docking study was carried out by the Autodock Vina.[29,30] The optimized structures of compounds **1–4** (b3lyp/6-311++G(d,p)) were used for the docking calculations. The crystal structure of Kinase ThiM from *Klebsiella pneumoniae* was downloaded from the protein data bank (PDB 6k28), the water molecules and heteroatoms were removed, the polar hydrogen atoms were added, and the Gasteiger charges were applied to the protein structure. All chains were deleted except chain A. The search space was determined using GetBox PyMOL plugin using the cocrystallized TZE molecule at the center, yielding a box with center at 22.5, 63.5, 35.4, and dimensions of 15.5, 14.6, 15.1. Docking automation was carried out using PyRx 0.8 (**https://link.springer.com/protocol/10.1007/978-1-4939-2269-7_19**). Figures were generated using UCSF Chimera 1.13.1 (**https://onlinelibrary.wiley.com/doi/10.1002/jcc.20084**) and PoseView (**https://academic.oup.com/bioinformatics/article/22/14/1710/226866?login=false**) (**https://pubs.acs.org/doi/10.1021/ci049958u**).

3 Results and discussion

3.1 Synthesis and characterization of molecules 1–4

The synthesis of thiadiazole derivatives **1–4** was carried out using a mixture of methoxy cinnamic acid and phenylthiosemicarbazide derivatives in presence of phosphorous oxychloride (Fig. 2).

Compound	R_1	R_2
1	5-OCH_3	NO_2
2	6-OCH_3	NO_2
3	5-OCH_3	CH_3
4	6-OCH_3	CH_3

^{13}C-NMR, ^{1}H-NMR, and FT-IR, spectroscopies and elemental analysis were performed to determine the structure of the molecules **1–4**.

The FT-IR spectrum of molecules **1**, **2**, **3** and **4** shows bands in range 3262–3167 cm^{-1} due to the stretching of N–H and C–H_{Ar} groups and the bands in range 1575–1183 cm^{-1} are attributed to C=N, C–N and C–S stretching vibrations.

N–H proton between phenyl and thiadiazole ring resonated at δ_H 9.94, 9.95, 10.45 and 10.47 ppm, respectively for the molecules **1**, **2**, **3** and **4**. The signals observed as multiple bands are between δ 8.43–7.00, 8.41–7.02, 7.27–7.00, and 7.55–7.16 ppm respectively for the molecules **1**, **2**, **3** and **4**, due to aromatic protons.

In the ^{13}C-NMR spectra, the two characteristic peaks of the two carbons of 1,3,4-thiadiazole ring are at 163.5–158.4, 164.23–160.1, and 164.0 and 159.4 ppm for molecules **1**, **2** and **3**, respectively. The two peaks at δ 163.8 and 160.1 ppm were the characteristic peaks of two carbons of 1,3,4-thiadiazole ring, and the other ^{13}C-NMR (DMSO) spectrum data of molecule **4** showed 118.2–158.0 (10C, aromatic carbons), 112.3 and 115.5 (alkenic carbons), and 55.62 (1C, –OCH_3) for molecule **1**.

In order to investigate the structures' geometry, DFT calculations were performed. The DFT calculations at b3lyp/6-311++G(d,p) level in the gas phase showed that all the structures were linear as the dihedral angles C7–C8–C9–S13 and C12–N10–C21–C22 were close to 0° (Fig. 3). Fig. 4 depicts the frontier orbital calculations of compounds **1–4**.[31] For all molecules, the HOMO orbitals were distributed over the aromatic skeleton, while the LUMO orbitals of molecules **1** and **2** were positioned

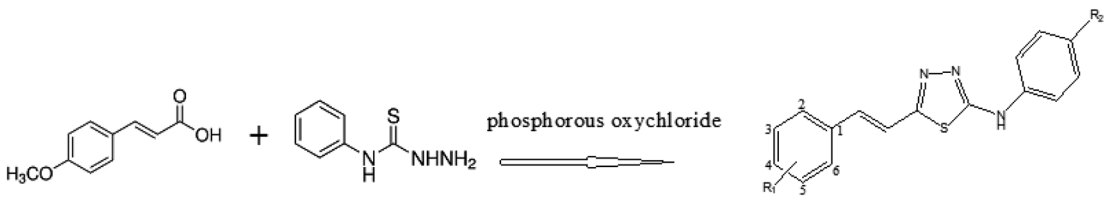


Fig. 2 The structure of the synthesized thiadiazole derivatives.

© 2022 The Author(s). Published by the Royal Society of Chemistry

Open Access Article. Published on 17 October 2022. Downloaded on 10/31/2022 3:10:04 PM.
This article is licensed under a Creative Commons Attribution-NonCommercial 3.0 Unported Licence.

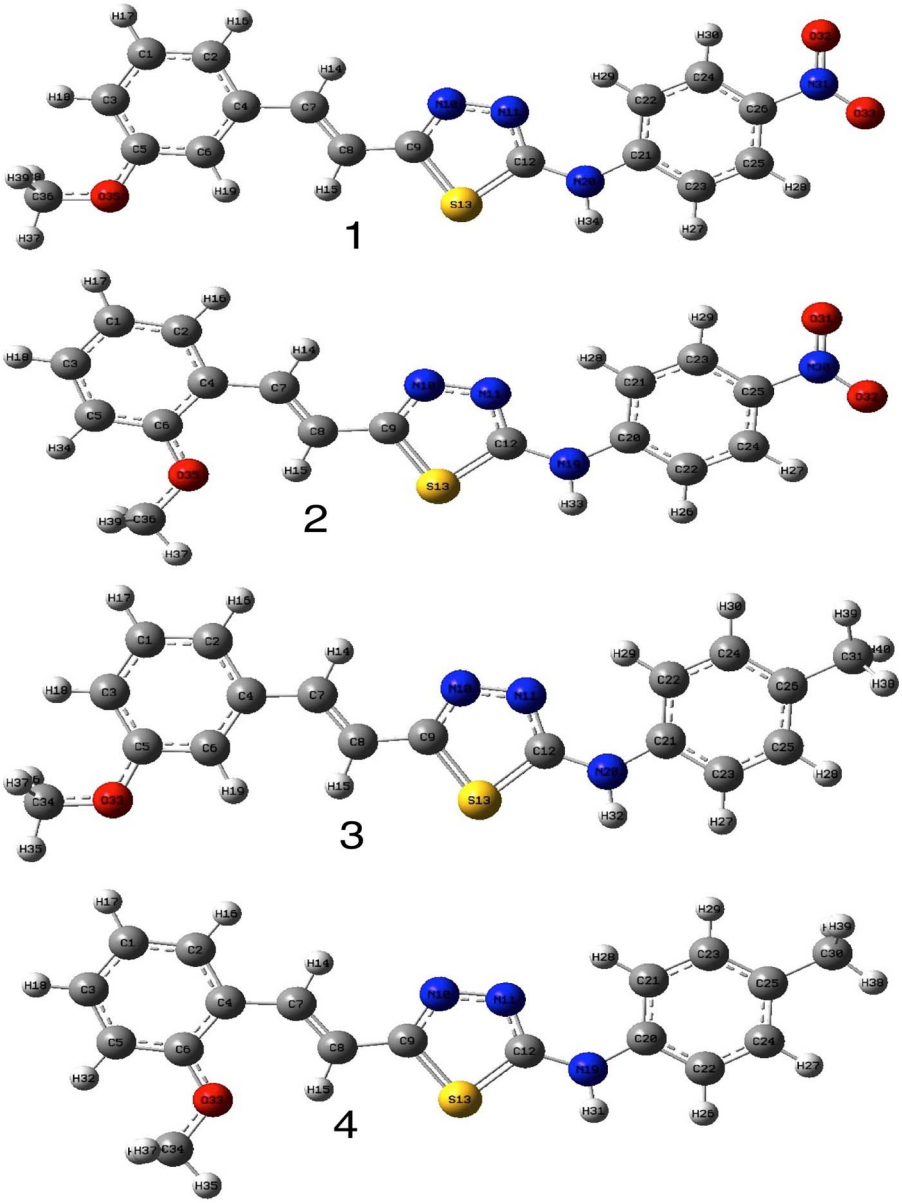


Fig. 3 Optimized structures of compounds **1–4** at b3lyp/6-311++G(d,p) level of theory in the gas phase.

on the NO_2-ph unit. The substituted $-CH_3$ group changed the situation, where the LUMO orbitals were distributed over the thiadiazole ring. Table 1 summarizes the calculated HOMO, LUMO, and energy gap values for the investigated compounds. The calculated HOMO energies revealed that values were in the order of **1** > **2** > **3** > **4**. These results indicate that compound **1** is the most reactive ligand towards the interactions with protein receptors.[32,33] The calculated energy gap of the investigated molecules showed that compound **1** and **2** featured the lower values, indicating lower reactivity of the two molecules.

Molecular electrostatic surface potential (MESP) of molecules is an important factor to describe the active site of ligands.[34–37] The MESP of **1–4** molecules were calculated using the optimized structures at b3lyp/6-311++G(d,p) level of theory to explore the nucleophilic and electrophilic sites on the ligands' surface. Fig. 4 indicates that the positive regions (nucleophilic sites) were positioned on the –NH group, while the negative regions (electrophilic sites) were situated over the thiadiazole and NO_2 group in compounds **1** and **2**, and the thiadiazole unit dominated the electrophilic attack in compounds **2** and **4**. Ionization potential and electron affinity of the investigated molecules were used to assess the reactivity parameters of compounds **1–4**. The calculated IP and EA of the investigated compounds showed that compound **1** has the highest affinity to donate and accept electrons from the receptors, while compound **4** is the weakest electron donor (Table 2). This result indicates the high polarizability of compound **1** as compared to the other ligands. The calculated ω^- and ω^+ values confirmed the high electron mobility of the molecules in the order **1** > **2** > **3** > **4**. The calculated chemical hardness of the

Open Access Article. Published on 17 October 2022. Downloaded on 10/31/2022 3:10:04 PM.
This article is licensed under a Creative Commons Attribution-NonCommercial 3.0 Unported Licence.

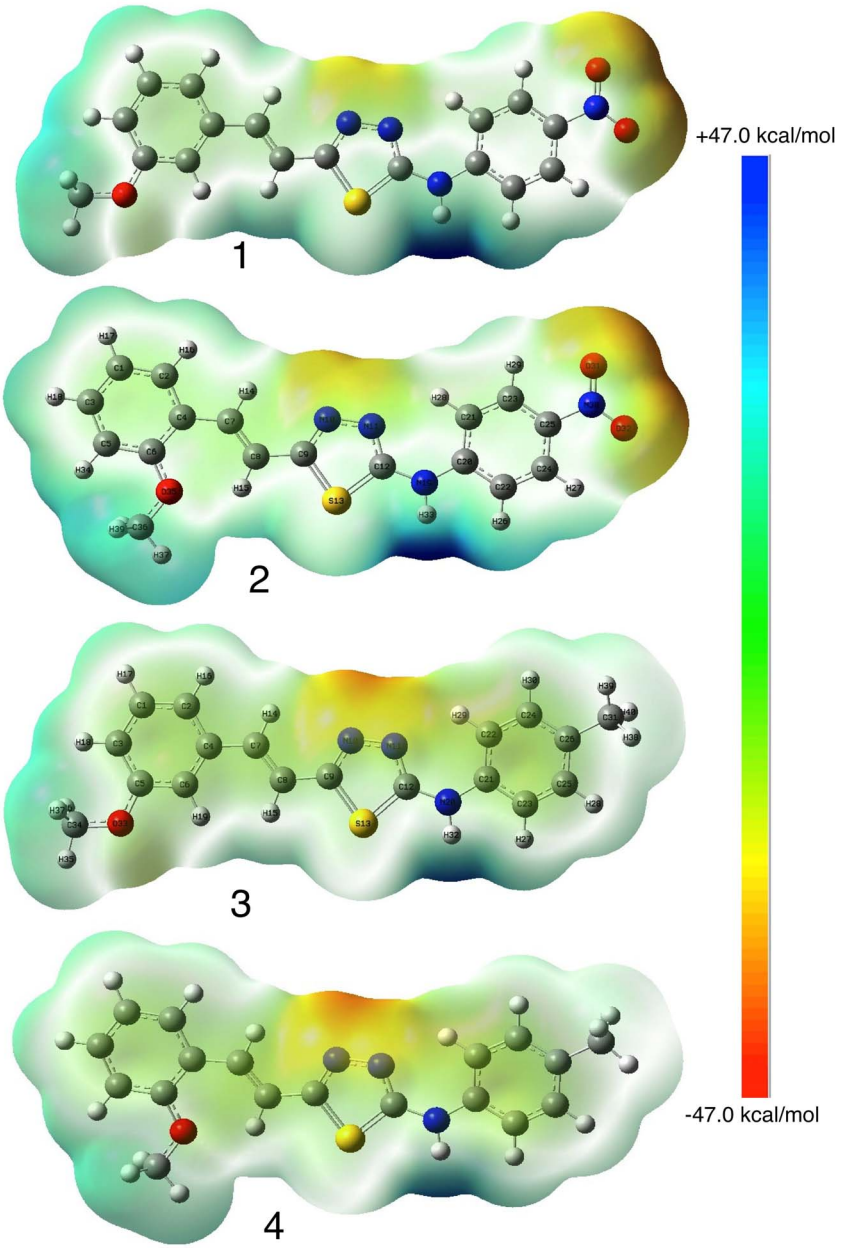


Fig. 4 Calculated MESP of compounds **1–4**.

investigated molecules suggested that compound **1** and **2** have the lowest values, which indicates the facile charge transfer process.

3.2 Antimicrobial activity

In vitro biological screening tests for antimicrobial activity of the synthesized 1,3,4-thiodiazole molecules were performed against various Gram-positive and Gram-negative bacterial strains. The Gram-negative bacteria consist of *Salmonella kentucky*, *Enterobacter aerogenes* ATCC 13048, *Klebsiella pneumoniae*, *Escherichia coli*, *Proteus*, and *Pseudomonas aeruginosa*. The Gram-positive bacteria investigated are *Enterococcus faecium*, *Listeria monocytogenes* ATCC 7644, ATCC 25923, *Staphylococcus aureus*, *Enterococcus durans*, *Serratia marcescens*, *Staphylococcus aureus* ATCC, *Staphylococcus epidermidis*, alfa *Streptococcus haemolyticus*, *Staphylococcus hominis*, and *Enterococcus faecium*. Additionally, antifungal activity was tested using *Candida albicans* ATCC 26555. Antimicrobial studies were carried out by the disk diffusion method and the tests were performed in triplicate. No zone of inhibition was observed in the tests performed with the molecules **1–4** at 0.2 M against Gram-positive (*Listeria monocytogenes* ATCC 7644, *S. aureus* ATCC, monocytogenes *E. faecium*, *S. aureus* ATCC 25923, *E. durans*, *S. marcescens*, *E. faecium*), Gram negative (*S. kentucky*, *E. aerogenes* ATCC 13048, *P. aeruginosa*, *K. pneumoniae*, *E. coli*, *Proteus*) and the fungi *C. albicans* ATCC 26555 (Table 3).

© 2022 The Author(s). Published by the Royal Society of Chemistry

Open Access Article. Published on 17 October 2022. Downloaded on 10/31/2022 3:10:04 PM.
This article is licensed under a Creative Commons Attribution-NonCommercial 3.0 Unported Licence.

Table 1 Calculated HOMO and LUMO orbitals of compounds **1–4** in the gas phase at b3lyp/6-311++G(d,p)

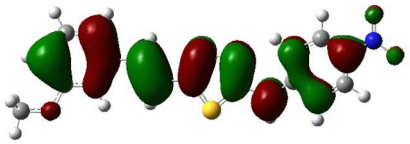
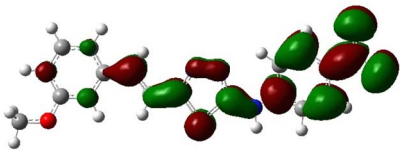
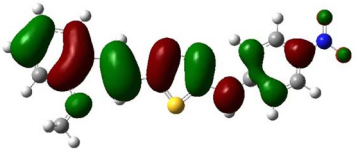
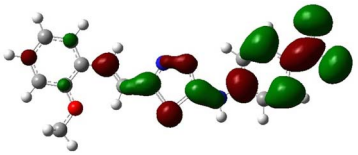
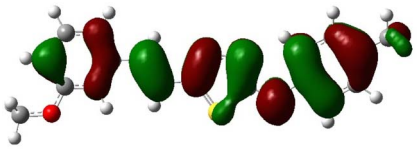
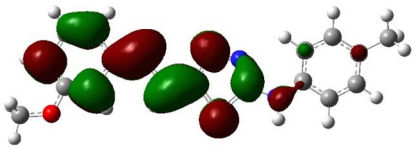
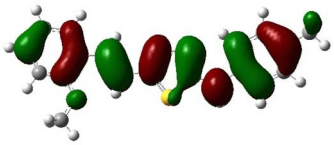
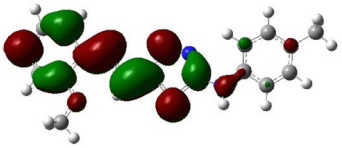
	HOMO	LUMO
1		
2		
3		
4		

Table 2 Calculated frontier orbital energies, energy gap, ionization potential, electron affinity (EA, eV), chemical hardness (η, eV), electron donating power (ω^-, eV), and electron acceptor power (ω+, eV)

	1	2	3	4
E_{HOMO} (eV)	−6.15	−5.99	−5.59	−5.47
E_{LUMO} (eV)	−2.73	−2.67	−2.07	−1.92
E_g (eV)	3.42	3.32	3.52	3.55
IP (eV)	6.15	5.99	5.59	5.47
EA (eV)	2.73	2.67	2.07	*1.92*
η (eV)	3.42	3.32	3.52	*3.55*
ω^- (eV)	8.20	8.02	6.30	*5.91*
ω^+ (eV)	2.58	2.56	2.01	*1.90*

Molecules **1–4** displayed inhibition zone on Gram-positive *S. hominis*, *S. epidermidis*, alfa *S. haemolyticus* and Gram-negative *K. pneumoniae* (Fig. 5).

The difference between molecules **1** and **2** is that the methoxy group is in the *ortho* position in molecule **1** and the *meta* position in molecule **2**. When the methoxy group was in the *ortho* position, an inhibition zone of approximately 8 mm was obtained for *S. hominis* and 6 mm for *S. epidermidis*, *K. pneumoniae* and alpha *S. haemolyticus*. When the methoxy group was in the *meta* position, an inhibition zone of about 8 and 9 mm on *S. hominis* and *K. pneumoniae* were recorded, respectively, while no effect on *S. epidermidis* and alpha *S. haemolyticus* was observed (Fig. 6).

The difference between molecules **1** and **3** is that the methyl group, which is the electron donating group, is attached to the phenyl ring instead of the nitro group, which is the electron withdrawing group.

Molecule **3**, to which electron donor groups were bound, exhibited the highest zone of inhibition on *S. epidermis* (19 mm), *S. hominis* (17 mm), *K. pneumoniae* (14 mm) and alfa *S. haemolyticus* (8 mm). El-Sheshtawy *et al.*[37] synthesized the complex [$TiCl_2$(bzac)(L4)] and reported that is more potent against *S. typhimurium*, *E. aerogenes*, *S. epidermidis*, *S. aureus*, and *M. luteus* with 13, 13, 15, 15, and 16.5 mm zone inhibition diameters, respectively. Raj Kaushal *et al.* also indicated that titanium(IV) complex can bind to calf thymus DNA (CT-DNA) *via* an intercalative mode.[38]

Molecule **4** revealed the biggest inhibition zone for *K. pneumoniae* (14 mm) followed by *S. hominis* (8 mm), *S. epidermidis* (6 mm) and alfa *S. haemolyticus* (6 mm).

In order to investigate the potential activity of the investigated compounds as inhibitors, the molecular docking of the four compounds was performed. The 5-(hydroxyethyl)-methylthiazole kinase (*ThiM*) of *Klebsiella pneumoniae* has a key role in bacterial thiamine and salvage pathway. It is essential in the pathway forming thiamine pyrophosphate (TPP) which is and essential co-factor in bacterial amino acid and carbohydrate metabolic pathways. It is considered an attractive antibacterial target due to its absence in humans. Hence, molecular docking study was carried out on *ThiM* (PDB 6k28) to investigate the compounds inhibitory activity to *Klebsiella pneumoniae*.

The molecular docking results were reported as 9 poses for each ligand with the corresponding ligand-protein binding

Open Access Article. Published on 17 October 2022. Downloaded on 10/31/2022 3:10:04 PM.
This article is licensed under a Creative Commons Attribution-NonCommercial 3.0 Unported Licence.

Table 3 Inhibition zone of the synthesized compounds **1–4** at a concentration of 0.2 M

No.	Type of bacteria	Compound **1**	Compound **2**	Compound **3**	Compound **4**
1	*Klebsiella pneumoniae*	6 mm	9 mm	14 mm	14 mm
2	*Staphylococcus aureus* ATCC	—	—	—	—
3	*Staphylococcus aureus*	—	—	—	—
4	*Proteus*	—	—	—	—
5	*E. coli*	—	—	—	—
6	*Serratia marcescens*	—	—	—	—
7	*Staphylococcus hominis*	8 mm	8 mm	17 mm	8 mm
8	*Staphylococcus epidermidis*	6 mm	—	19 mm	6 mm
9	Alfa *Streptococcus haemolyticus*	6 mm	—	8 mm	6 mm
10	*Enterococcus faecium*	—	—	—	—
11	*Pseudomonas aeroginosa*	—	—	—	—
12	*Listeria monocytogenes* ATCC 7644	—	—	—	—
13	*Enterococcus faecium*	—	—	—	—
14	*Enterococcus durans*	—	—	—	—
15	*Salmonella kentucky*	—	—	—	—
16	*Enterobacter aerogenes* ATCC 13048	—	—	—	—
17	*Candida albicans* ATCC 26555	—	—	—	—

affinity. Docking poses were chosen based on the alignment of the compounds' thiadiazole ring over the co-crystallized ligand thiazole ring. The docking results showed docking affinity values for the complex of −6.9, −6.9, −7.1, and −7 kcal mol^{-1} for compounds **1**, **2**, **3**, and **4**, respectively. This result indicates that compound **3** has the highest affinity towards the *Klebsiella*

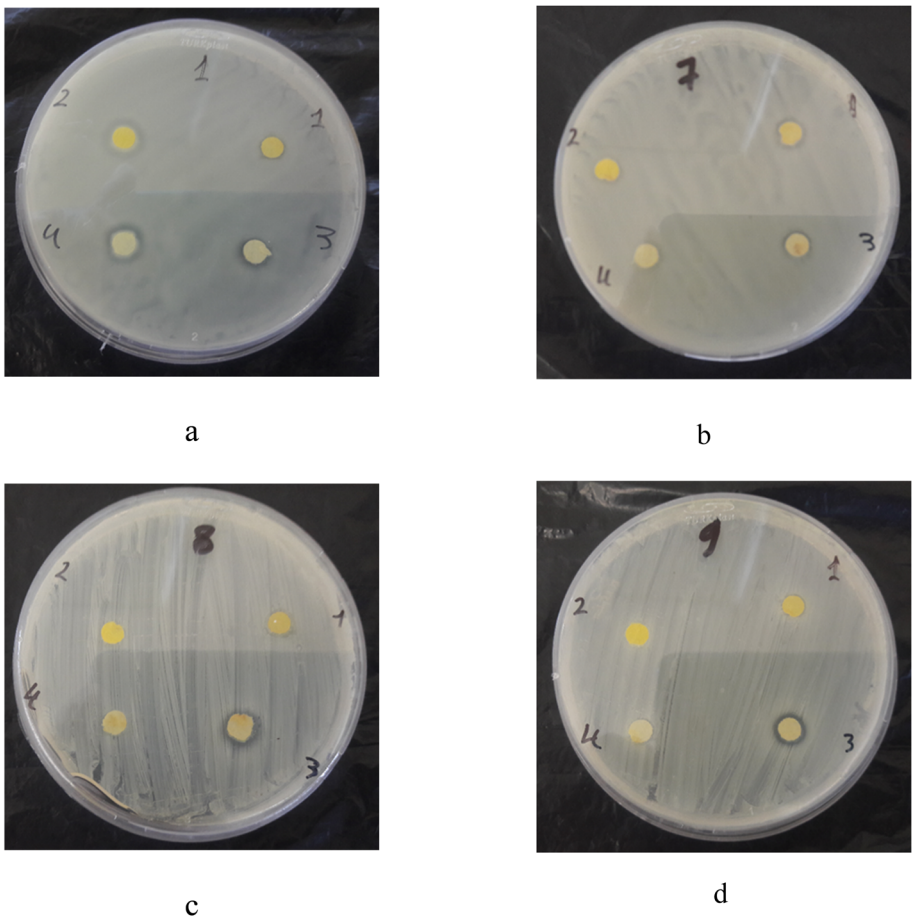


Fig. 5 Inhibition zone of **1–4** compounds on (a) *Klebsiella pneumoniae*, (b) *Staphylococcus hominis*, (c) *Staphylococcus epidermidis*, (d) alfa *Streptococcus haemolyticus*.

© 2022 The Author(s). Published by the Royal Society of Chemistry

Open Access Article. Published on 17 October 2022. Downloaded on 10/31/2022 3:10:04 PM.
This article is licensed under a Creative Commons Attribution-NonCommercial 3.0 Unported Licence.

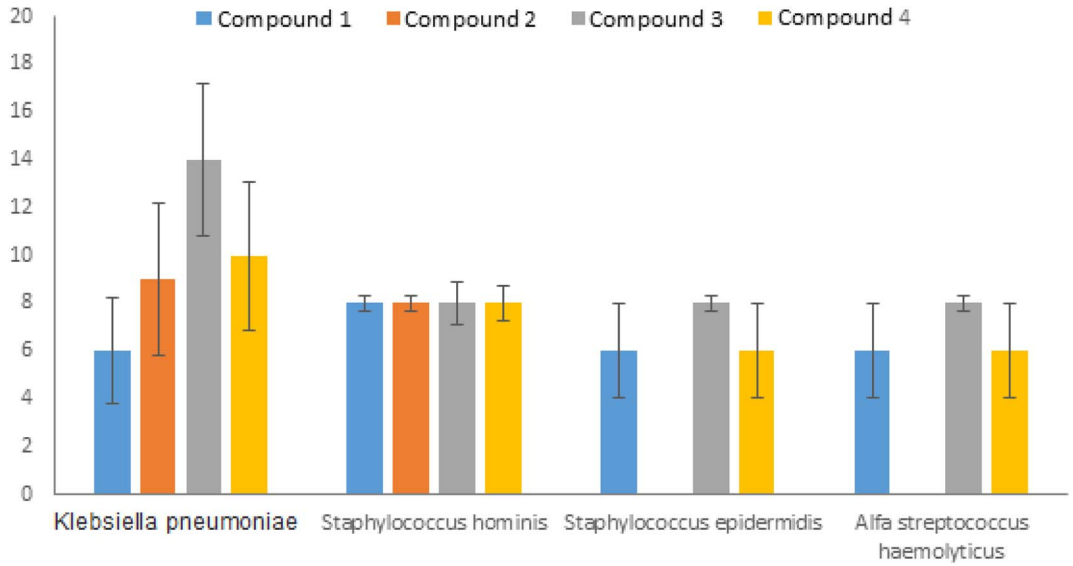


Fig. 6 Inhibition zone for compounds on a: *Klebsiella pneumoniae*, *Staphylococcus hominis*, *Staphylococcus epidermidis*, and alfa *Streptococcus haemolyticus*.

pneumoniae followed by **4**, then **2** and **1**, which is in accordance with the experimental results.

The ligand–protein interactions for compounds **1** and **2** are shown in Fig. 7. In Fig. 7a, Compound **1** is stabilized inside the binding site by a main conventional hydrogen bond between its nitro group and Arg 108 residue of chain B. Another hydrogen bond with Pro 47 of chain A is formed by the compound's amino group. Compound **1** also forms and additional pi–sulphur

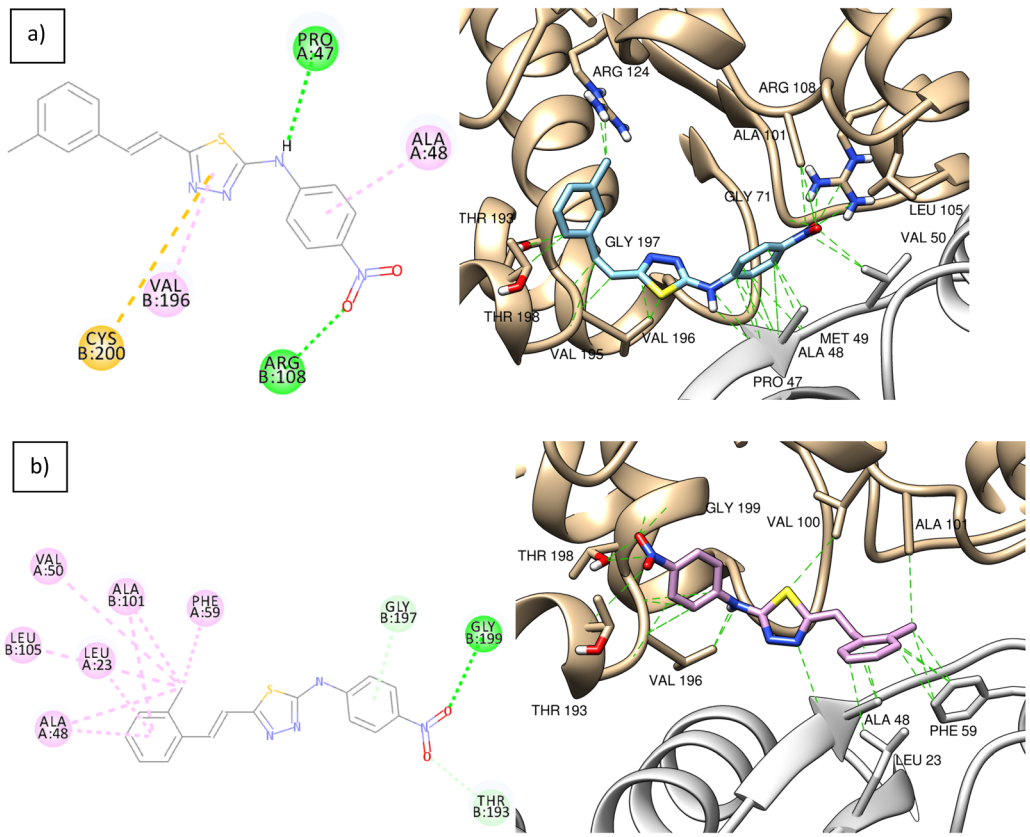


Fig. 7 (a) 2D (left) and 3D (right) interactions of compound **1** inside the protein's active site, (b) 2D (left) and 3D (right) interactions of compound **2** inside the protein's active site. Hydrophobic interactions in green dashed lines. Chain A and chain B in grey and khaki colours, respectively.

Open Access Article. Published on 17 October 2022. Downloaded on 10/31/2022 3:10:04 PM.
This article is licensed under a Creative Commons Attribution-NonCommercial 3.0 Unported Licence.

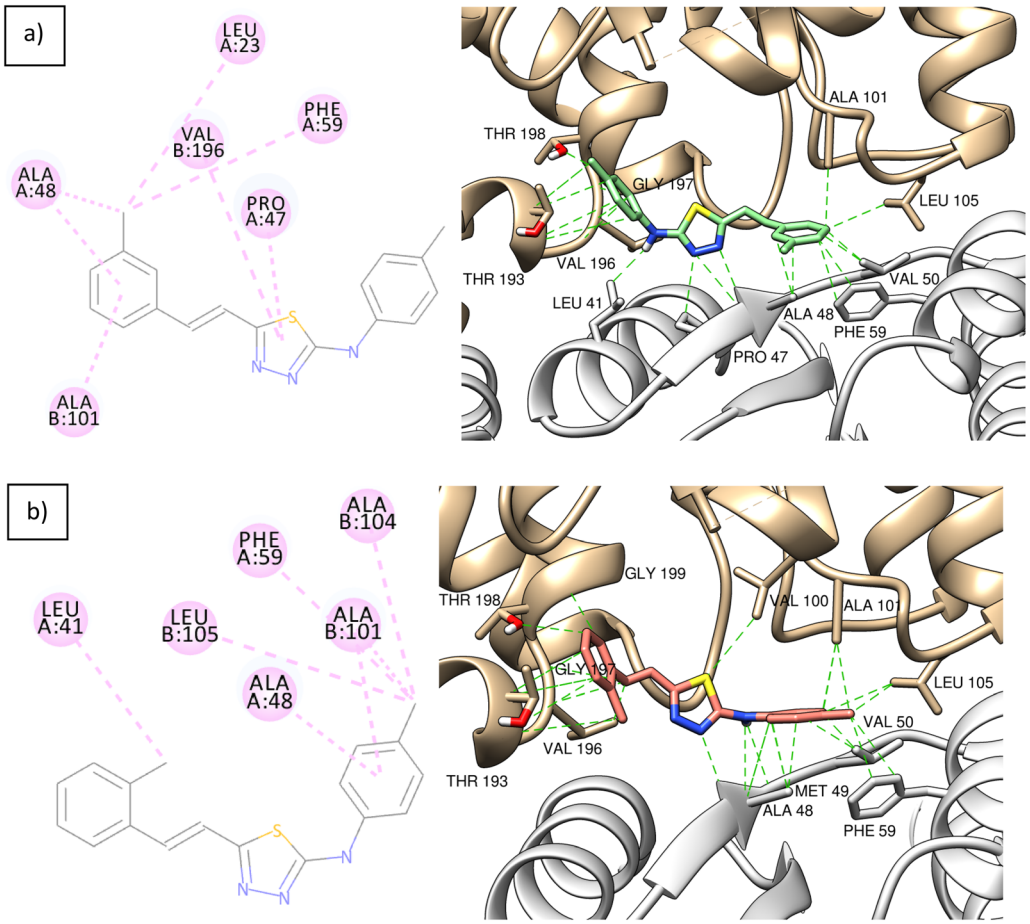


Fig. 8 (a) 2D (left) and 3D (right) interactions of compound **3** inside the protein's active site, (b) 2D (left) and 3D (right) interactions of compound **4** inside the protein's active site. Hydrophobic interactions in green dashed lines. Chain A and chain B in grey and khaki colours, respectively.

interaction with its thiadiazole pi system and sulphur group of Cys 200 residue of chain B. Compound **2** forms; a hydrogen bond by its nitro group with Gly 199 residue of chain B. In Fig. 7b, the compound is also stabilized with hydrophobic interactions formed between the compound's *o*-phenyl group with the protein's hydrophobic pocket formed by residues of Leu 23, Ala 48, Val 50, and phenylalanine 59 residues of chain A, and Ala 101 and Leu 105 residues of chain B.

The ligand–protein interactions of compounds **3** and **4** are shown in Fig. 8. Both compounds are stabilized inside the binding site by hydrophobic interactions. In Fig. 8a, compound **3** forms hydrophobic interactions by its *m*-phenyl group with the hydrophobic pocket formed by residues of alanine 101 and leucine 105 of chain A, and proline 47, alanine 48, valine 50, and phenylalanine 59 of chain B. In Fig. 8b, compound **4** also forms hydrophobic interactions with the same hydrophobic pocket through its *p*-phenyl group.

3.3 CT-DNA binding

In this section, the binding of the synthesized ligand molecules (**1–4**) with CT-DNA was assessed by UV-Vis absorption. Generally, DNA plays an important role in the life process as it contains all the genetic information for cellular function. However, DNA molecules are prone to damage under a variety of conditions, such as interactions with certain molecules. This damage can lead to various pathological changes in living organisms since the DNA binding interaction of molecules is of interest for both therapeutic and scientific reasons.[39] Absorption spectroscopy is an effective method to examine the binding mode of DNA with micromolecules. Because of compound binding to DNA, the absorbance spectrum shows hypochromism and hyperchromism, which involve a strong stacking interaction between an aromatic chromophore and the base pairs of DNA.[40] Thus, in order to provide evidence for the possibility of binding of synthesized ligand molecules (**1–4**) with CT-DNA, spectroscopic titration of solutions of the CT-DNA with synthesized ligand molecules (**1–4**) have been performed and the binding constants have been calculated by absorption spectra using Benesi–Hildebrand equation. In general, the hyperchromism and hypochromism were regarded as spectral features for DNA double-helix structural change when DNA reacted with other molecules. The hyperchromism means the breakage of the secondary structure of DNA; the hypochromism originates from the stabilization of the DNA duplex by either the intercalation-binding mode or the electrostatic effect of small molecules.[33] The absorption spectra of the constant

© 2022 The Author(s). Published by the Royal Society of Chemistry

Open Access Article. Published on 17 October 2022. Downloaded on 10/31/2022 3:10:04 PM.
This article is licensed under a Creative Commons Attribution-NonCommercial 3.0 Unported Licence.

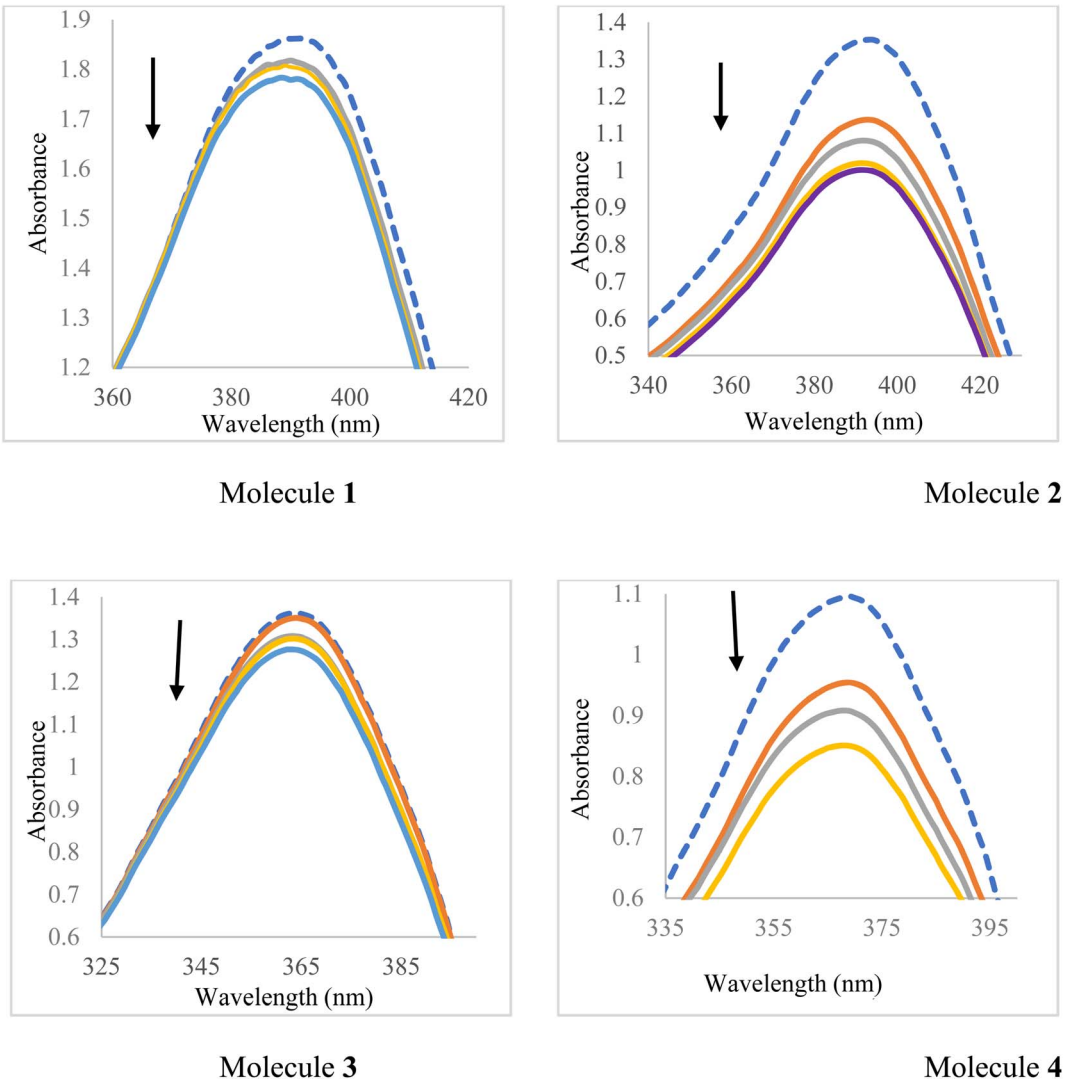


Fig. 9 Absorbance of molecules 1–4 in the presence and absence of CT-DNA.

concentration (40 μM) of the synthesized ligand molecules (**1–4**) upon addition of different concentration of CT-DNA are shown in Fig. 9. It is apparent from Fig. 9 that the absorption peak of the synthesized ligand molecules (**1–4**) around at 390 nm, 393 nm, 360 nm, 367 nm, respectively, showed gradual decrease with the increasing concentration of CT-DNA. This was attributed to the electrostatic interaction between the DNA and the small molecules. Slight hypsochromic shifts can be explained by the increasing of energy between π and π* due to repulsion between the non-bonding, electrons localized on the hetero atoms (N, S and O) in both CT-DNA base pairs and the synthetized molecules. The increasing of the energy gap between π and π* explained the low absorptivity of the synthesized molecules in the presence of CT-DNA.[16] This explanation is agreed with the values of binding constant K_b of molecules **1–4** are 5.4×10^4, 5.5×10^4, 1.5×10^4 and 3×10^4, respectively. When the methyl group (electron donor group) attached to the phenyl ring instead of the electron withdrawing NO_2 group, there is a decrease in the binding constant value. The more repulsion is occurred between the non-bonding electrons in case of the molecules with electron donating groups due to the electron density has been increased on the heteroatoms in the organic ligands.[40–54]

4 Conclusions

To sum up, 5-[(*E*)-2-(3-methoxyphenyl)]vinyl-*N*-[4′-nitrophenyl]-1,3,4-thiadiazole-2-amine (**1**), 5-[(*E*)-2-(2-methoxyphenyl)]vinyl-*N*-[4′-nitrophenyl]-1,3,4-thiadiazole-2-amine (**2**), 5-[(*E*)-2-(3-methoxyphenyl)]vinyl-*N*-[4′-methylphenyl]-1,3,4-thiadiazole-2-amine (**3**), and 5-[(*E*)-2-(2-methoxyphenyl)]vinyl-*N*-[4′-methylphenyl]-1,3,4-thiadiazole-2-amine (**4**) were synthesised. The DFT calculations have been used to explore the geometric and spectroscopic properties of the molecules. Derivatives **1–4** showed good antibacterial activity against *Klebsiella pneumoniae* and *Staphylococcus hominis*, where **1**, **3** and **4** were more effective against *Staphylococcus epidermidis* and alfa *Streptococcus haemolyticus*. The docking study on *Kinase ThiM* from *Klebsiella*

Open Access Article. Published on 17 October 2022. Downloaded on 10/31/2022 3:10:04 PM. This article is licensed under a Creative Commons Attribution-NonCommercial 3.0 Unported Licence.

pneumoniae shows the formation of hydrogen bonding with the receptor residue, which confirms the inhibition effect of the ligands. The collected results revealed that molecules **1–4** interact with CT-DNA by intercalative mechanism. The binding ability study of the synthesized molecules with CT-DNA revealed that nitro groups attached to the phenyl group slightly increased the binding constant compared to methyl groups.

Conflicts of interest

There are no conflicts to declare.

Acknowledgements

The authors would like to thank Princess Nourah bint Abdulrahman University Researchers Supporting Project number (PNURSP2022R9), Princess Nourah bint Abdulrahman University, Riyadh, Saudi Arabia for supporting this project.

References

1 U. Kalidhar and A. Kaur, 1,3,4-Thiadiazole derivatives and their biological activities: A review, *Res. J. Pharm., Biol. Chem. Sci.*, 2011, **2**, 1091–1106.
2 S. Georgeta, S. Oana, S. Eugenia and B. Sanda, 2-Amino-1,3,4-thiadiazole as a potential scaffold for promising antimicrobial agents, *Drug Des., Dev. Ther.*, 2018, **12**, 1545–1566.
3 S. Haider, M. S. Alam and H. Hamid, 1,3,4-Thiadiazoles: A potent multi targeted pharmacological scaffold, *Eur. J. Med. Chem.*, 2015, **92**, 156–177.
4 M. Amir, A. Kumar, I. Ali and S. A. Khan, Synthesis of pharmaceutically important 1,3,4-thiadiazole and imidazolinone derivatives as antimicrobials, *Indian J. Chem.*, 2009, **48B**, 1288–1293.
5 J. Salimon, N. Salih, A. Hameed, H. Ibraheem and E. Yousif, Synthesis and antibacterial activity of some new 1,3,4-oxadiazole and 1,3,4-thiadiazole derivatives, *J. Appl. Sci. Res.*, 2010, **6**(7), 866–870.
6 E. E. Oruc, S. Rollas, F. Kandemirli, N. Shvets and A. Dimoglo, 1,3,4-Thiadiazole derivatives. Synthesis, structure elucidation and structure-antituberculosis activity relationship investigation, *J. Med. Chem.*, 2004, **47**(27), 6760–6767.
7 S. Schenone, C. Brullo, O. Bruno, *et al.*, New 1,3,4-thiadiazole derivatives endowed with analgesic and anti-inflammatory activities, *Bioorg. Med. Chem.*, 2006, **14**(6), 1698–1705.
8 L. Labanauskas, V. Kalcas, E. Udrenaite, P. Gaidelis, A. Brukstus and A. Dauksas, Synthesis of 3-(3,4-dimethoxy phenyl)-1*H*-1,2,4-triazole-5-thiol and 2-amino-5-(3,4-dimethoxy phenyl)-1,3,4-thiadiazole derivatives exhibiting anti-inflammatory activity, *Pharmazie*, 2001, **56**, 617–619.
9 H. Khalilullah, M. U. Khan, D. Mahmood, J. Akhtar and G. O. Elhassan, 1,3,4-Thiadiazole: A biologically active scaffold, *Int. J. Pharm. Pharm. Sci.*, 2014, **6**, 8–15.
10 S. R. Pattan, N. S. Desai, P. A. Rabara, A. A. Bukitgar and V. A. Wakale, Synthesis and antimicrobial evaluation of some 1,3,4-thiadiazole derivatives, *Indian J. Pharm. Educ. Res.*, 2008, **42**(4), 314–318.
11 A. Basso, M. Liu, C. Dai, *et al.*, SCH 2047069, a novel oral kinesin spindle protein inhibitor, shows single-agent antitumor activity and enhances the efficacy of chemotherapeutics, *Mol. Cancer Ther.*, 2010, **9**(11), 2993–3002.
12 S. S. Taha, A. A. Ahmad, S. I. Mawlood and N. O. Ali, Synthesis of some series of 2-amino-1,3,4-thiadiazole derivatives with their pathogenic bacterial activity, *J. Raparin Univ.*, 2017, **4**(11), 63–78.
13 A. A. Kadi, E. S. Al-Abdullah, I. A. Shehata, E. E. Habib, T. M. Ibrahim and A. A. El-Emam, Synthesis, antimicrobial and anti-inflammatory activities of novel 5-(1-adamantyl)-1,3,4-thiadiazole derivatives, *Eur. J. Med. Chem.*, 2010, **45**(11), 5006–5011.
14 M. Gür, M. Muğlu, M. S. Çavuş, A. Güder, H. S. Sayiner and F. Kandemirli, Synthesis, characterization, quantum chemical calculations and evaluation of antioxidant properties of 1,3,4-thiadiazole derivatives including 2-and 3-methoxy cinnamic acids, *J. Mol. Struct.*, 2017, **1134**, 40–50.
15 A. A. Othman, M. Kihel and S. Amara, 1,3,4-Oxadiazole, 1,3,4-thiadiazole and 1,2,4-triazole derivatives as potential antibacterial agents, *Arabian J. Chem.*, 2014, **12**, 1660–1675.
16 J. Y. Chou, S. Y. Lai, S. L. Pan, G. M. Jow, J. W. Chern and J. H. Guh, Investigation of anticancer mechanism of thiadiazole-based compound in human nonsmall cell lung cancer A549 cells, *Biochem. Pharmacol.*, 2003, **66**, 115–124.
17 A. Kaur, R. Kumar and U. Kalidhar, Synthesis, spectral studies and biological activity of some novel biphenyl imidazo[2,1-b][1,3,4]thiadiazole derivatives, *Res. J. Pharm., Biol. Chem. Sci.*, 2012, **3**, 1084–1096.
18 S. Georgeta, S. Oana, S. Eugenia and B. Sanda, *Drug Des., Dev. Ther.*, 2018, **12**, 1545–1566.
19 N. Kushwaha, S. K. S. Kushwaha and A. K. Rai, Biological activities of thiadiazole Derivatives: A Review, *Int. J. Chem. Res.*, 2012, **4**, 517–531.
20 T. A. Farghaly, M. A. Abdallah and M. R. A. Aziz, Synthesis and antimicrobial activity of some new 1,3,4-thiadiazole derivatives, *Molecules*, 2012, **17**, 14625–14636.
21 R. Bhatia and A. Kaur, Synthesis, spectral studies and antimicrobial activity of some imidazo [2,1-b] [1,3,4] thiadiazole derivatives, *Der Pharma Chem.*, 2014, **6**, 114–120.
22 O. E. Ozkan, G. Zengin, M. Akça, M. C. Baloğlu, Ç. Olgun, E. M. Altuner, S. Ateş, A. Aktümsek and H. Vurdu, DNA protection, antioxidant, antibacterial and enzyme inhibition activities of heartwood and sapwood extracts from juniper and olive woods, *RSC Adv.*, 2015, **5**, 72950–72958.
23 N. Sharath, S. Halehatty, B. Naik, B. N. Kumar and J. Hoskeri, Antibacterial, molecular docking, DNA binding and photocleavage studies on novel heterocyclic pyrazoles, *Br. J. Pharm. Res.*, 2011, **1**, 46–65.
24 P. Pakravan and S. Masoudian, Study on the interaction between isatin-β-thiosemicarbazone and Calf Thymus DNA by spectroscopic techniques, *Iran. J. Pharm. Res.*, 2015, **14**, 111–123.

© 2022 The Author(s). Published by the Royal Society of Chemistry

Open Access Article. Published on 17 October 2022. Downloaded on 10/31/2022 3:10:04 PM. This article is licensed under a Creative Commons Attribution-NonCommercial 3.0 Unported Licence.

25 N. Hadjiliadis and E. Sletten, *Metal complex–DNA interactions*, Blackwell Publishing Ltd, 2009, pp. 138–129, https://onlinelibrary.wiley.com/doi/book/10.1002/9781444312089.
26 H. A. Benesi and J. H. Hildebrand, A spectrophotometric investigation of the interaction of iodine with aromatic hydrocarbons, *J. Am. Chem. Soc.*, 1949, **71**, 2703–2707.
27 M. J. Frisch, G. W. Trucks, H. B. Schlegel, G. E. Scuseria, M. A. Robb, J. R. Cheeseman, G. Scalmani, V. Barone, B. Mennucci and G. A. Petersson, *Gaussian 09, Revision d1*, Inc., Wallingford, CT, USA, 2009.
28 J. L. Gázquez, A. Cedillo and A. Vela, Electrodonating and Electroaccepting Powers, *J. Phys. Chem. A*, 2007, **111**, 1966–1970.
29 O. Trott and A. J. Olson, AutoDock Vina: Improving the speed and accuracy of docking with a new scoring function, efficient optimization, and multithreading, *J. Comput. Chem.*, 2010, **31**, 455–461.
30 K. Schöning-Stierand, K. Diedrich, R. Fährrolfes, F. Flachsenberg, A. Meyder, E. Nittinger, R. Steinegger and M. Rarey, ProteinsPlus: interactive analysis of protein–ligand binding interfaces, *Nucleic Acids Res.*, 2020, **48**, W48–W53.
31 R. Fährrolfes, S. Bietz, F. Flachsenberg, A. Meyder, E. Nittinger, T. Otto, A. Volkamer and M. Rarey, ProteinsPlus: a web portal for structure analysis of macromolecules, *Nucleic Acids Res.*, 2017, **45**, W337–W343.
32 M. Er, B. Ergüven, H. Tahtaci, A. Onaran, T. Karakurt and A. Ece, Synthesis, characterization, preliminary SAR and molecular docking study of some novel substituted imidazo[2,1-b][1,3,4]thiadiazole derivatives as antifungal agents, *Med. Chem. Res.*, 2017, **26**, 615–630.
33 M. Er, A. Özer, Ş. Direkel, T. Karakurt and H. Tahtaci, Novel substituted benzothiazole and Imidazo[2,1-b][1,3,4] Thiadiazole derivatives: Synthesis, characterization, molecular docking study, and investigation of their in vitro antileishmanial and antibacterial activities, *J. Mol. Struct.*, 2019, **1194**, 284–296.
34 H. S. El-Sheshtawy and I. El-Mehasseb, Role of halogen and hydrogen bonds for stabilization of antithyroid drugs with hypohalous acids (HOX, X = I, Br, and Cl) adducts, *J. Mol. Struct.*, 2017, **1147**, 643–650.
35 Q.-L. Zhang, J.-G. Liu, H. Chao, G.-Q. Xue and L.-N. Ji, DNA binding and photocleavage studies of cobalt(III) polypyridyl complexes: $[Co(phen)_2IP]^{3+}$ and $[Co(phen)_2PIP]^{3+}$, *J. Inorg. Biochem.*, 2001, **83**(1), 49–55.
36 H. S. El-Sheshtawy, M. M. Ibrahim, I. El-Mehasseb and M. El-Kemary, Orthogonal hydrogen/halogen bonding in 1-(2-methoxyphenyl)-1H-imidazole-2(3H)-thione-I2 adduct: An experimental and theoretical study, *Spectrochim. Acta, Part A*, 2015, **143**, 120–127.
37 H. S. El-Sheshtawy, H. M. A. Salman and M. El-Kemary, Halogen vs Hydrogen Bonding in Thiazoline-2-thione Stabilization with σ- and π-Electron Acceptors Adducts: Theoretical and Experimental study, *Spectrochim. Acta, Part A*, 2015, **137**, 442–449.
38 R. Kaushal, S. Thakur and K. Nehra, ct-DNA Binding and Antibacterial Activity of Octahedral Titanium (IV) Heteroleptic (Benzoylacetone and Hydroxamic Acids) Complexes, *Int. J. Med. Chem.*, 2016, 2361214.
39 H. S. El-Sheshtawy, M. M. Ibrahim, M. R. E. Aly and M. El-Kemary, Spectroscopic and structure investigation of the molecular complexes of tris(2-aminoethyl)amine with π-acceptors, *J. Mol. Liq.*, 2016, **213**, 82–91.
40 M. S. Attia, M. N. Ramsis, L. H. Khalil and S. G. Hashem, *J. Fluoresc.*, 2012, **22**, 779–788.
41 M. S. Attia, A. O. Youssef, Z. A. Khan and M. N. Abou-Omar, *Talanta*, 2018, **186**, 36–43.
42 M. S. Attia, A. O. Youssef and A. A. Essawy, *Anal. Methods*, 2012, **4**, 2323–2328.
43 M. S. Attia, K. Ali, M. El-Kemary and W. M. Darwish, *Talanta*, 2019, **201**, 185–193.
44 M. S. Attia, W. H. Mahmoud, A. O. Youssef and M. S. Mostafa, *J. Fluoresc.*, 2011, **21**, 2229–2235.
45 M. S. Attia, M. H. Khalil, M. S. A. Abdel-Mottaleb, M. B. Lukyanova, Yu. A. Alekseenko and B. Lukyanov, *Int. J. Photoenergy*, 2006, 1–9.
46 M. S. Attia, W. H. Mahmoud, M. N. Ramsis, L. H. Khalil, A. M. Othman, S. G. Hashem and M. S. Mostafa, *J. Fluoresc.*, 2011, **21**, 1739–1748.
47 M. S. Attia, A. M. Othman, E. Elraghi and H. Y. Aboul-Enein, *J. Fluoresc.*, 2011, **21**, 739–745.
48 A. A. Elabd and M. S. Attia, *J. Lumin.*, 2016, **169**, 313–318.
49 M. S. Attia, S. A. Elsaadany, K. A. Ahmed, M. M. El-Molla and M. S. A. Abdel-Mottaleb, *J. Fluoresc.*, 2015, **25**, 119–125.
50 S. G. Hashem, M. M. Elsaady, H. G. Afify, M. El-Kemary and M. S. Attia, *Talanta*, 2019, **199**, 89–96.
51 M. S. A. Abdel-Mottaleb, M. Saif, M. S. Attia, M. M. Abo-Aly and S. N. Mobarez, *Photochem. Photobiol. Sci.*, 2018, **17**, 221–230.
52 W. E. Omer, M. A. El-Kemary, M. M. Elsaady, A. A. Gouda and M. S. Attia, *ACS Omega*, 2020, **5**, 5629–5637.
53 L. M. Abdullah, M. S. Attia and M. S. A. Abdel-Mottaleb, *Egypt. J. Chem.*, 2019, **62**, 247–255.
54 M. S. Attia, A. O. Youssef, A.-S. S. H. Elgazwy, S. M. Agami and S. I. Elewa, *J. Fluoresc.*, 2014, **24**, 759–765.

© 2022 The Author(s). Published by the Royal Society of Chemistry